



HAL
open science

Coumarin derivatives as versatile photoinitiators for 3D printing, polymerization in water and photocomposite synthesis

Mira Abdallah, Akram Hijazi, Bernadette Graff, Jean-Pierre Fouassier, Giacomo Rodeghiero, Andrea Gualandi, Frederic Dumur, Pier Giorgio Cozzi, Jacques Lalevee

► To cite this version:

Mira Abdallah, Akram Hijazi, Bernadette Graff, Jean-Pierre Fouassier, Giacomo Rodeghiero, et al.. Coumarin derivatives as versatile photoinitiators for 3D printing, polymerization in water and photocomposite synthesis. *Polymer Chemistry*, 2019, 10 (7), pp.872–884. 10.1039/c8py01708e . hal-02491514

HAL Id: hal-02491514

<https://hal.science/hal-02491514>

Submitted on 8 Jul 2020

HAL is a multi-disciplinary open access archive for the deposit and dissemination of scientific research documents, whether they are published or not. The documents may come from teaching and research institutions in France or abroad, or from public or private research centers.

L'archive ouverte pluridisciplinaire **HAL**, est destinée au dépôt et à la diffusion de documents scientifiques de niveau recherche, publiés ou non, émanant des établissements d'enseignement et de recherche français ou étrangers, des laboratoires publics ou privés.

Coumarin derivatives as versatile photoinitiators for 3D printing, polymerization in water and photocomposite synthesis

Mira Abdallah^{1,2,3}, Akram Hijazi³, Bernadette Graff^{1,2}, Jean-Pierre Fouassier^{1,2}, Giacomo Rodeghiero,⁴ Andrea Gualandi,⁴ Frederic Dumur,^{*5} Pier Giorgio Cozzi,^{*4} Jacques Lalevée^{*1,2}

¹Université de Haute-Alsace, CNRS, IS2M UMR 7361, F-68100 Mulhouse, France

²Université de Strasbourg, France

³EDST, Université Libanaise, Campus Hariri, Hadath, Beyrouth, Liban.

⁴ALMA MATER STUDIORUM Università di Bologna, Dipartimento di Chimica "G. Ciamician", Via Selmi2, 40126 Bologna, Italy

⁵ Aix Marseille Univ, CNRS, ICR UMR 7273, F-13397 Marseille, France

Corresponding author: jacques.lalevee@uha.fr; Frederic.dumur@univ-amu.fr,

piergiorgio.cozzi@unibo.it

ABSTRACT:

The goal of this paper concerns the first evaluation of two recently reported coumarins to initiate photopolymerization reactions. These two compounds (CoumA and CoumB) are proposed as high performance visible light photoinitiators and evaluated as photoredox catalysts (PCs), in the presence of an iodonium salt or with an amine, for both the free radical polymerization (FRP) of (meth)acrylates and the cationic polymerization (CP) of epoxides upon visible light exposure using LED at 405 nm. These coumarin derivatives showed a high photoinitiation ability i.e. excellent polymerization rates and high final monomer conversions were obtained. The photophysical and photochemical properties of the coumarin derivatives were studied in terms of absorption, steady state photolysis and fluorescence spectroscopy. The photoinitiation mechanisms of the coumarin derivatives were discussed from fluorescence quenching, redox behavior and cyclic voltammetry experiments. A full picture of the involved photochemical mechanisms is provided. Coumarin-based systems being high performance photoinitiators, their

use in new photosensitive 3D printing resins will be also presented. Remarkably, CoumB is also found to be very efficient for the preparation of hydrogels in mild conditions due to its high solubility in water i.e. CoumB corresponds to a **high-performance** water soluble photoinitiator. Finally, the usage of the new coumarin derivatives for photocomposites synthesis with glass fibers (thick samples with good depth of cure) using Near-UV conveyor (LED @395 nm) is particularly outlined.

KEYWORDS: Coumarin; photocomposites; photopolymerization; photoredox catalysts; water soluble photoinitiators; 3D printing resins.

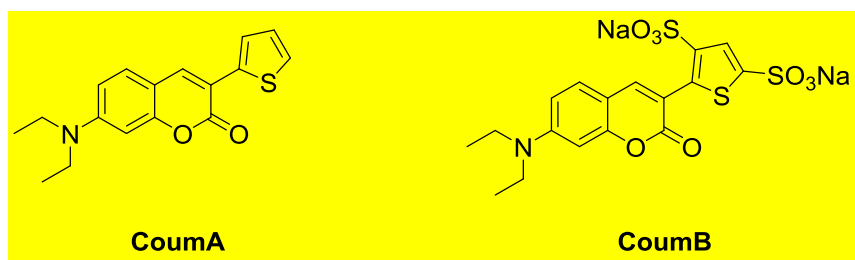
1. INTRODUCTION

Fluorescent heterocyclic compounds are point of interest in many disciplines such as emitters for electroluminescence devices [1], molecular probes for biochemical research [2] but also as dyes in traditional textile and polymer fields [3], fluorescent whitening agents [4] and photo conducting materials [5]. In this domain, coumarins and their derivatives are well-known fluorescent compounds with high quantum yields. Coumarins derivatives have been largely employed as fluorescent bio labels [6a], laser dyes [6b], emitting materials in organic light-emitting diodes (OLED) [6c], and dyes in solar cells [6d]. Coumarin derivatives have been also reported as: i) sensitizers for free radical polymerization (FRP) under UV light [7], ii) photoinitiators (PI) for Free-Radical-Initiated Photoimaging Systems under UV light [8], and iii) organic photoredox catalysts (PCs) [9], thanks to their wide variety of electronic, photochemical and photophysical properties. In addition, their straightforward synthesis [10] give the possibility

to vary their photophysical and redox properties [11], allowing to cover a wide range of photochemical properties and redox potentials.

The novelty of our work is the use of new synthesized coumarin derivatives (recently reported by one of us (PGC) as photoredox catalysts (PCs) in organic chemistry) in high performance photoinitiating systems for both the free radical polymerization (FRP) of (meth)acrylates and the cationic polymerization (CP) of epoxides using mild irradiation conditions. These coumarin derivatives will be incorporated into two-component (PI/iodonium salt (Iod) or PI/amine (NPG or EDB)) and three-component (PI/Iod/NPG) photoinitiating systems (PISs) to generate the reactive species (radicals or cations) able to initiate both FRP and CP processes upon near-UV or visible light (LED @375 nm, and LED @405 nm). A detailed analysis of their absorption properties, steady state photolysis, molecular orbitals, excited state processes and production of initiating species will be presented, and the structure/reactivity/efficiency relationships will be also discussed in detail.

To highlight their high performance in photoinitiating systems, their use in photosensitive 3D printing resins will be shown as well as the formation of hydrogels using the water soluble photoinitiator character of CoumB. Hydrogels have recently drawn great attention for use in a wide variety of biomedical applications such as cell therapeutics, wound healing, cartilage/bone regeneration and the sustained release of drugs. This is due to their biocompatibility and the similarity of their physical properties to natural tissue [12]. Currently, hydrogels are used for manufacturing contact lenses, hygiene products, tissue engineering scaffolds and drug delivery systems [13-15]. The manufacture of thick glass fibers/(meth)acrylate resin composites using the coumarin derivatives is also shown, and the preparation of the composites is discussed too.



Scheme 1. Investigated Compounds.

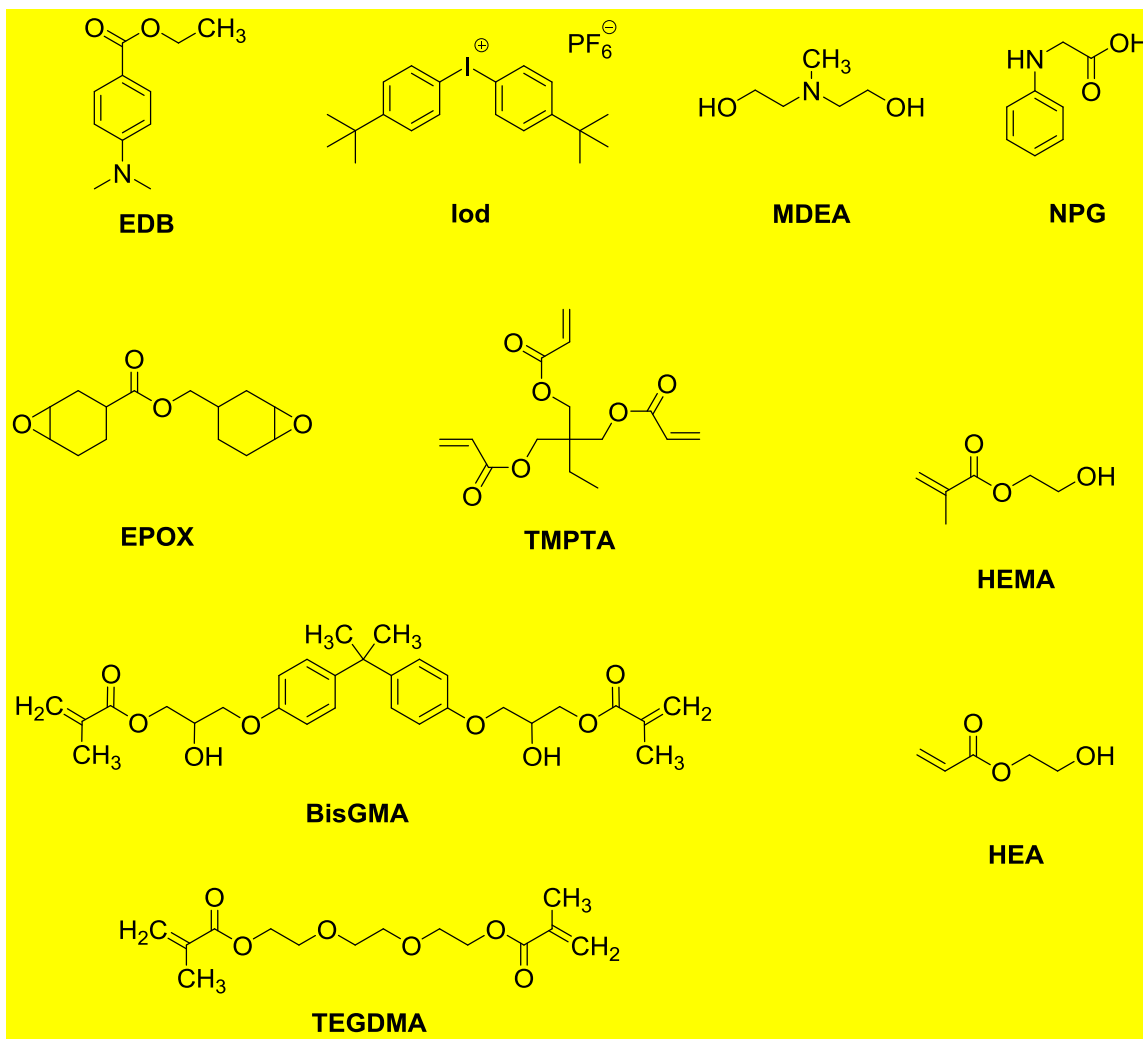
2. EXPERIMENTAL PART

2.1. Synthesis of CoumA and CoumB

The procedure for the synthesis of CoumA and CoumB is given in [9].

2.2. Other chemical compounds

All the other chemical compounds were selected with highest purity available and used as received, they are given in Scheme 2. Di-*tert*-butyl-diphenyl iodonium hexafluorophosphate (Iod or SpeedCure 938) was obtained from Lambson Ltd. *N*-Methyldiethanolamine (MDEA) was obtained from Alfa Aesar. *N*-phenylglycine (NPG), Ethyl-4-(dimethylamino)benzoate (EDB), bisphenol A-glycidyl methacrylate (BisGMA), triethyleneglycol dimethacrylate (TEGDMA) and 2-(hydroxyethyl) acrylate (HEA) were obtained from Sigma Aldrich. 2-(Hydroxyethyl) methacrylate (HEMA) was obtained from Tokyo Chemical Industry. (3,4-epoxycyclohexane)methyl 3,4-epoxycyclohexylcarboxylate (EPOX; Uvacure 1500) and trimethylolpropane triacrylate (TMPTA) were obtained from Allnex. TMPTA (or BisGMA/TEGDMA) and EPOX were selected as benchmarked resins for radical and cationic polymerization, respectively.



Scheme 2. Other Used Chemical Compounds

2.3. Irradiation Sources

The following Light Emitting Diodes (LEDs) were used as irradiation sources: i) LED @375 nm with an incident light intensity at the sample surface: $I_0 = 40 \text{ mW.cm}^{-2}$; ii) LED @405 nm; $I_0 = 110 \text{ mW.cm}^{-2}$; iii) LED projector @405 nm for 3D printing; $I = 100\text{-}130 \text{ mW.cm}^{-2}$.

2.4. Cationic Photopolymerization (CP) and Free Radical Photopolymerization (FRP)

The two-component photoinitiating systems (PISs) are mainly based on Coumarin/Iodonium salt or Coumarin/Amine (NPG or EDB) [(0.2%/1% w/w) or (0.5%/1% w/w)] for FRP and/or CP. The three-component photoinitiating systems (PISs) are mainly based on Coumarin/Iodonium salt/NPG [(0.2%/1%/1% w/w)] for FRP. The weight percent of the different chemical compounds of the photoinitiating system is calculated from the monomer content (w/w). The photosensitive thin formulations (~25 μm of thickness) were deposited on a BaF_2 pellet under air for the CP of EPOX, while for the FRP of TMPTA it was done in laminate (the formulation is sandwiched between two polypropylene films to reduce the O_2 inhibition). The 1.4 mm thick samples of (meth)acrylates were also polymerized under air into a rounded plastic mold of ~ 7 mm diameter and 1.4 mm of thickness. For thin samples, the evolution of the epoxy group content of EPOX and the double bond content of acrylate functions were continuously followed by real time FTIR spectroscopy (JASCO FTIR 4100) at about 790 and 1630 cm^{-1} , respectively. The evolution of the (meth)acrylate characteristic peak for the thick samples (1.4 mm) was followed in the near-infrared range at ~6160 cm^{-1} . The procedure used to monitor the photopolymerization profiles has been described in detail in refs [16,17,18].

2.5. Redox Potentials

The redox potentials for CoumA and CoumB (E_{ox} and E_{red}) were measured in acetonitrile by cyclic voltammetry with tetrabutylammonium hexafluorophosphate (0.1 M) as the supporting electrolyte (potential vs. Saturated Calomel Electrode). The free energy change ΔG_{et} for an electron transfer reaction was calculated from equation (eq. 1) [19] where E_{ox} , E_{red} , E_{S} , and C are the oxidation potential of the electron donor, the reduction potential of the electron acceptor, the excited state energy level (determined from luminescence experiments) and the Coulombic term for the initially formed ion pair, respectively. C is neglected as usually done in polar solvents.

$$\Delta G_{\text{et}} = E_{\text{ox}} - E_{\text{red}} - E_{\text{S}} + C \quad (\text{eq 1})$$

2.6. ESR Spin-Trapping (ESR-ST) Experiments

The ESR-ST experiments were carried out using an X-Band spectrometer (Magnettech MS400). A LED@405 nm was used as irradiation source for triggering the production of radicals at room temperature (RT) under N₂ in *tert*-butylbenzene and trapped by phenyl-*N-tert*-butylnitrone (PBN) according to a procedure described elsewhere in details in [17,18]. The ESR spectra simulations were carried out with the PEST WINSIM program.

2.7. UV-Visible absorption and Photolysis Experiments

The UV-Visible absorbance properties of the compounds as well as the steady state photolysis experiments were studied using JASCO V730 UV–visible spectrometer.

2.8. Fluorescence Experiments

The fluorescence properties of the compounds were studied using a JASCO FP-6200 spectrofluorimeter.

2.9. Computational Procedure

Molecular orbital calculations were carried out with the Gaussian 03 suite of programs [20,21]. The electronic absorption spectra for the different compounds were calculated with the time-dependent density functional theory at the MPW1PW91-FC/6-31G* level of theory on the relaxed geometries calculated at the UB3LYP/6-31G* level of theory. The triplet state energy levels were calculated at this level of theory.

2.10. 3D Printing Experiments

For 3D printing experiments, a laser diode @405 nm (spot size around 50 μm) and also a LED projector @405 nm (Thorlabs) were used for the spatially controlled irradiation. Rather similar intensities on the surface of the sample and similar emission spectrum for the laser diode or the LED used in 3D printing and the RT-FTIR kinetic experiments were used for sake of comparison. The photosensitive resin (various thickness) was polymerized under air and the generated patterns were analyzed by a numerical optical microscope (DSX-HRSU from OLYMPUS Corporation) as presented in [22,23].

2.11. Hydrogel formation

The formation of hydrogels was carried out in 50% water/50% HEMA (or HEA) in which the water soluble photoinitiating system was added (CoumB with an amine such as *N*-methyldiethanolamine MDEA). A LED @405 nm was used as irradiation source for the formation of hydrogels in the absence of air, at room temperature (RT) after degassing the mixture with nitrogen. The generated hydrogels were analyzed by thermogravimetric analysis (TGA).

2.12. Near-UV conveyor

The Dymax-UV conveyor was used to cure composites. The glass fibers were impregnated with the organic resin (50/50 w/w%) and then irradiated. The UV conveyor is equipped with a 120 mm wide Teflon-coated belt and one UV lamp (mercury–Fe doped lamp). The distance between the lamp and the belt can be manually adjusted (fixed at 15 mm) as can the belt speed (fixed at 2 $\text{m}\cdot\text{min}^{-1}$). LED@395nm is another source of light used as alternative ($4\text{W}/\text{cm}^2$).

3. RESULTS AND DISCUSSION

3.1. Light Absorption Properties of the Investigated Compounds

The UV-Visible absorption spectra of CoumA and CoumB in acetonitrile are reported in Figure 1. These compounds are characterized by very high molar extinction coefficients (ϵ) both in the near UV and the visible range (e.g. CoumA, $\epsilon = 35200 \text{ M}^{-1}.\text{cm}^{-1}$ at $\lambda_{\text{max}} = 421 \text{ nm}$, and CoumB, $\epsilon = 28100 \text{ M}^{-1}.\text{cm}^{-1}$ at $\lambda_{\text{max}} = 405 \text{ nm}$, see also in Table 1). Remarkably, their absorptions are intense in the 270-510 nm spectral range, ensuring an excellent overlap with the emission spectra of the near UV or visible LEDs used in this work (e.g., @375 and @405 nm).

The optimized geometries as well as the frontier orbitals (Highest Occupied Molecular Orbital HOMO and Lowest Unoccupied Molecular Orbital LUMO) for CoumA and CoumB are given in Figure 2. Both the HOMO and LUMO are strongly delocalized all over the π -conjugated system in both compounds clearly showing a $\pi \rightarrow \pi^*$ lowest energy transition. The higher delocalization of both HOMO and LUMO overall the π scaffold in CoumA (vs. CoumB) is observed in agreement with a lower HOMO-LUMO gap leading to a bathochromic shift of $\approx 20 \text{ nm}$ for CoumA (vs. CoumB).

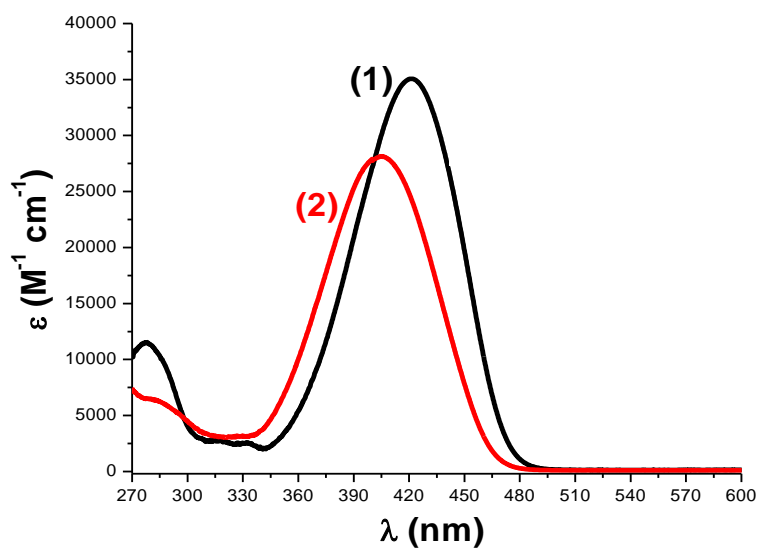


Figure 1. Absorption spectra of the investigated compounds in acetonitrile: (1) CoumA; and (2) CoumB.

Table 1. Light absorption properties of CoumA and CoumB: maximum absorption wavelengths λ_{max} , extinction coefficients at λ_{max} and extinction coefficients at the emission wavelength of the LED @405 nm.

PI	λ_{max} (nm)	ϵ_{max} ($M^{-1} \cdot \text{cm}^{-1}$)	$\epsilon_{(405\text{nm})}$ ($M^{-1} \cdot \text{cm}^{-1}$)
CoumA	421	35200	30600
CoumB	405	28100	28100

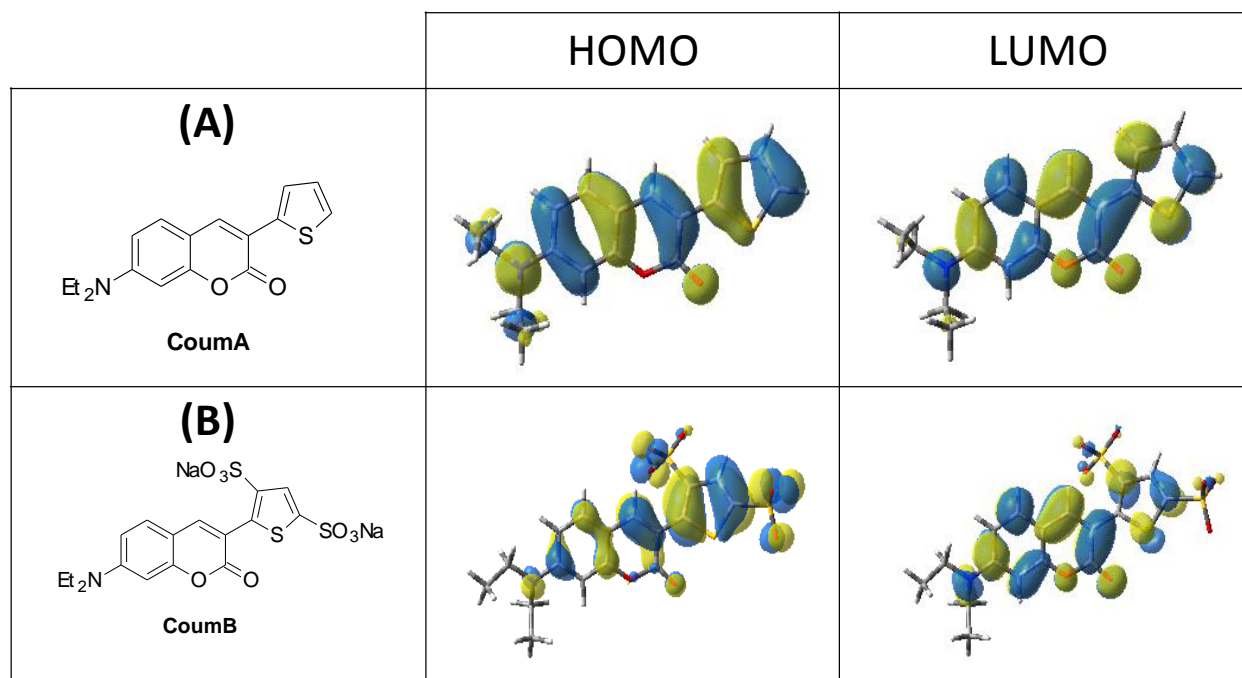


Figure 2. Contour plots of HOMOs and LUMOs for CoumA and CoumB; structures optimized at the B3LYP/6-31G* level of theory.

3.2. Cationic photopolymerization (CP) of Epoxides

A full study on the CP of epoxides (using EPOX as benchmarked monomer) in thin films (25 μm) was performed under air using the new compounds CoumA and CoumB.

Upon irradiation with LED @405 nm as a convenient soft irradiation source, the CP in the presence of two-component photoinitiating system based on CoumA/Iod system is very efficient in terms of R_p (rate of polymerization) and final epoxy function conversion (FC) (e.g. FC= 80% with 0.2% CoumA; Figure 3A, curve 1; Table 2). The same holds true but with slightly lower FC in the epoxy function at higher concentration of CoumA under the same irradiation conditions e.g. FC= 67% with 0.5% CoumA (w/w) compared to 80% with 0.2% CoumA (w/w); (Figure 3A, curve 2 vs curve 1, respectively; Table 2). This behavior can be attributed to the inner filter

effect i.e. the light penetration decreases for higher coumarin contents even for thin samples. In fact, it is well obvious that at higher concentrations, the color of the obtained thin polymer becomes darker and darker (Figure S1 in SI) in agreement with this inner filter.

For these irradiation conditions but using Iod alone, no polymerization occurs showing the huge effect of CoumA on the initiating ability. Therefore, CoumA can be considered as very good photoinitiator in combination with an iodonium salt (see the chemical mechanisms in part 3.7). In addition, a new peak ascribed to the formation of the polyether network during the photopolymerization reaction arises at $\sim 1080\text{ cm}^{-1}$ (see the FTIR spectra in the $750\text{-}1150\text{ cm}^{-1}$ range in Figures 3B for 0.2% CoumA, and 3C for 0.5% CoumA, respectively).

In the same context, CoumB/Iod system was tested but no polymerization was observed when using LED@405 nm under air (Figure 3A, curve 3) i.e., in Figure 3D, the polyether peak is not observed for CoumB/Iod compared with CoumA/Iod systems in Figure 3(B,C).

The efficiency trend for CP using LED@405 nm clearly follows the order CoumA \gg CoumB. This behavior can be partly connected to the absorption properties of the coumarin derivatives as CoumA being the most efficient PI and having higher extinction coefficient than CoumB. This behavior will be discussed below in details.

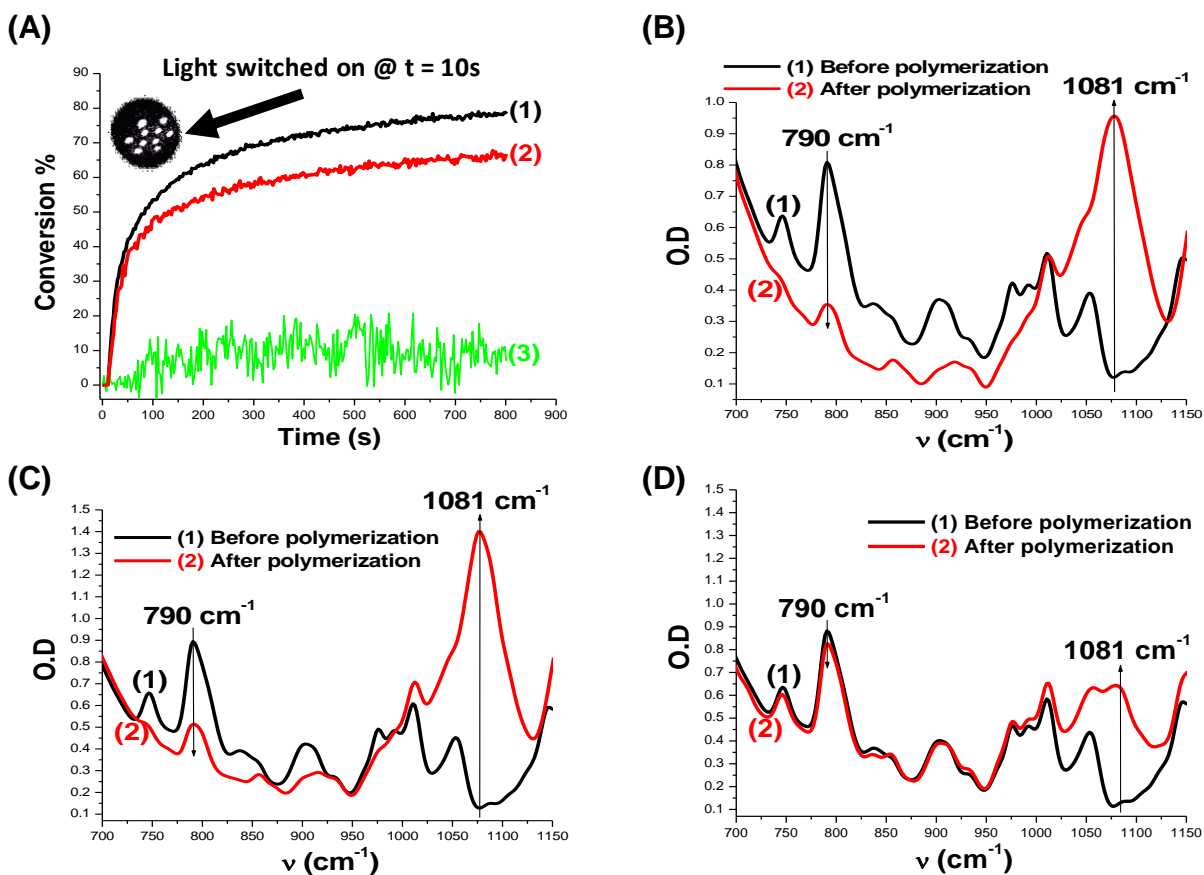


Figure 3. (A): Polymerization profiles (epoxy function conversion vs irradiation time) for EPOX under air (thickness = $25 \mu\text{m}$) upon exposure to LED@405 nm in the presence of the two-component photoinitiating systems: (1) CoumA/Iod (0.2%/1% w/w); (2) CoumA/Iod (0.5%/1% w/w); and (3) CoumB/Iod (0.2%/1% w/w). The irradiation starts for $t = 10$ s. (B): IR spectra recorded before and after polymerization for CoumA/Iod (0.2%/1% w/w) upon exposure to LED @405 nm. (C): IR spectra recorded before and after polymerization for CoumA/Iod (0.5%/1% w/w) upon exposure to LED @405 nm. (D): IR spectra recorded before and after polymerization for CoumB/Iod (0.2%/1% w/w) upon exposure to LED @405 nm.

Table 2. Final Reactive Epoxy Function Conversion (FC) for EPOX Using Different Photoinitiating Systems after 800 s of Irradiation with LED @405 nm.

Epoxy function conversion (FC) for EPOX (at t = 800 s); thin sample (25 μm) under air	
CoumA/Iod	CoumB/Iod
80% (0.2%/1% w/w); 67% (0.5%/1% w/w)	n.p. (0.2%/1% w/w)

n.p.: no polymerization

3.3. Free radical photopolymerization of acrylates (TMPTA)

Typical acrylate function conversion-time profiles for CoumA and CoumB based photoinitiating systems are given in Figure 4 and the FCs are summarized in Table 3. The FRP of TMPTA in thin films (25 μm), in laminate and in the presence of the CoumA/Iod or CoumA/Iod/NPG couples is quite efficient using the LED@405 nm (Figure 4A: curves 1 vs. 3, respectively). For CoumA, Iod or NPG alone, no or very low polymerization occurs showing the huge role of CoumA for the global performance of the system; this efficient behavior will be discussed later in details in the chemical mechanisms part.

In fact, CoumB/Iod couple is not able to initiate the FRP thin samples of acrylates under exposure to the LED@405 nm (Figure 4A, curve 5). This can be probably ascribed to their low initiating radical yield. This is also in agreement with its low initiating ability for CP (see above).

A photoredox catalyst behavior was observed upon using the Coumarin/Iod/NPG (0.2%/1%/1% w/w) three-component PISs under exposure to the LED@405 nm. The addition of the amine (NPG) as a hydrogen donor leads to an increase of the performance e.g., FC increases up to 56% with CoumA/Iod/NPG (0.2%/1%/1% w/w) compared to 40% with CoumA/Iod (0.2%/1% w/w) (Figure 4A, curve 3 vs curve 1, respectively - see also in Table 3). A Similar behavior is also observed with CoumB e.g., FC = 47% with CoumB/Iod/NPG (0.2%/1%/1%

w/w) compared to CoumB/Iod (0.2%/1% w/w), for which no polymerization has taken place (Figure 4A, curve 7 vs curve 5, respectively - see also in Table 3). In comparison, the two-component system Iod/NPG (1%/1% w/w) shows a mild polymerization profile (Figure 4A, curve 9), highlighting the crucial role of CoumA and CoumB.

In the same context, good polymerization profiles for the FRP of TMPTA in thick samples are also obtained when using LED@405 nm. The FRP of 1.4 mm thick samples of acrylates under air is very efficient in term of R_p (rate of polymerization) and final acrylate function conversion (FC) using two and three-component photoinitiating systems based on Coumarin/Iod (0.2%/1% w/w) and Coumarin/Iod/NPG combinations (0.2%/1%/1% w/w) upon irradiation with LED@405 nm, as shown in Figure 4B - see also in Table 3. For comparison, Iod alone was tested and no polymerization was observed using the same irradiation conditions, showing the role of CoumA or CoumB.

From our data, it is well obvious that CoumB/Iod PIS has higher final conversion of the acrylate functions than CoumA/Iod system (Figure 3B, curve 5 vs curve 1; see also in Table 3), this can be ascribed to the color of the obtained thick polymer that changed from fluorescent green to dark olive green in the case of the presence of CoumA/Iod as PIS leading to a strong inner filter effect during the polymerization; the phenomenon that is not observed in the presence of CoumB/Iod as PIS.

Remarkably, a tack free polymer is obtained when using CoumB as PI and exhibits good bleaching properties, while when using CoumA as PI the color of the obtained polymer remains dark suggesting rather poor bleaching properties during the polymerization (the photos of the thick films (1.4 mm) under air before and after polymerization are given in Figure S2).

Interestingly, when NPG is introduced in order to regenerate CoumA or CoumB in a three-component Coumarin/Iod/NPG systems (as demonstrated in Figure 4(B)), it was possible to obtain again a high performance for FRP in thick samples i.e. the efficiency is increased to reach 79% with CoumA/Iod/NPG (0.2%/1%/1% w/w) after 24s of irradiation instead of only 20% with CoumA/Iod (LED@405 nm; Figure 4B, curve 3 vs. curve 1, respectively). Similarly, with CoumB, a clear increase of the performance is also noted i.e. conversion of 87% after 13 s for CoumB/Iod/NPG (0.2%/1%/1% w/w) vs. 13% for CoumB/Iod (0.2%/1% w/w) (Figure 4B). In comparison, the two-component system Iod/NPG (1%/1% w/w) shows a good polymerization profile at least with LED@405 nm for FRP thick samples (Figure 4B, curve 9), but it shows a low rate of polymerization in comparison with those obtained by adding the coumarin derivatives (conversions of 79% with CoumA/Iod/NPG or 87% with CoumB/Iod/NPG after 24 s compared with Iod/NPG for which no polymerization occurs at this time of irradiation; Figure 4B curves 3&7, respectively compared to curve 9; see also in Table 3).

Using Coumarin/amine (such as NPG or EDB) (0.2%/1% w/w) systems, no polymerization was observed (curves (2),(4),(6) & (8) in Figures 4A&B). This can be probably ascribed to their low initiating radical yields that is not able to overcome the oxygen inhibition. This shows that, coumarin derivatives are probably poor photoinitiators in a photoreduction process (electron transfer from NPG or EDB to Coumarin) using an amine. CoumA and CoumB are more efficient in oxidation processes in combination with Iod (see above). The structure/reactivity/efficiency relationships will also be discussed below.

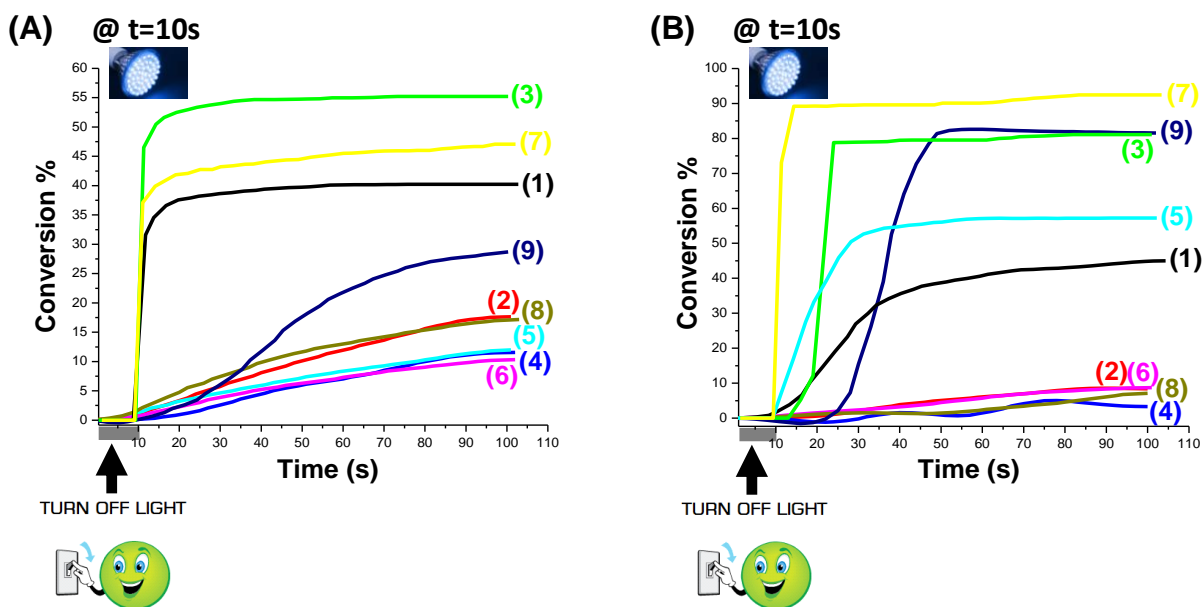


Figure 4. (A): Polymerization profiles of TMPTA (acrylate function conversion vs. irradiation time) in laminate (thickness = 25 μm) upon exposure to LED@405 nm in the presence of the two and three-component photoinitiating systems: (1) CoumA/Iod (0.2%/1% w/w); (2) CoumA/NPG (0.2%/1% w/w); (3) CoumA/Iod/NPG (0.5%/1%/1% w/w); (4) CoumA/EDB (0.2%/1% w/w); (5) CoumB/Iod (0.2%/1% w/w); (6) CoumB/NPG (0.2%/1% w/w); (7) CoumB/Iod/NPG (0.2%/1%/1% w/w); (8) CoumB/EDB (0.2%/1% w/w) and (9) Iod/NPG (1%/1% w/w); respectively. The irradiation starts for $t = 10$ s. **(B):** Polymerization profiles of TMPTA (acrylate function conversion vs. irradiation time) under air (thickness=1.4 mm) upon exposure to LED@405 nm in the presence of the two and three-component photoinitiating systems: (1) CoumA/Iod (0.2%/1% w/w); (2) CoumA/NPG (0.2%/1% w/w); (3) CoumA/Iod/NPG (0.5%/1%/1% w/w); (4) CoumA/EDB (0.2%/1% w/w); (5) CoumB/Iod (0.2%/1% w/w); (6) CoumB/NPG (0.2%/1% w/w); (7) CoumB/Iod/NPG (0.2%/1%/1% w/w); (8) CoumB/EDB (0.2%/1% w/w) and (9) Iod/NPG (1%/1% w/w); respectively. The irradiation starts for $t = 10$ s.

Table 3. Acrylate Function Conversion (FC) for TMPTA Using Different Photoinitiating Systems after 100s of Irradiation with LED @405 nm (A = CoumA; B = CoumB).

% acrylate function conversion (FC) for TMPTA (at t = 100 s); thin sample (25µm) in laminate								% acrylate function conversion (FC) for TMPTA (at t = 100 s); thick sample (1.4 mm) under air							
Two-component photoinitiating system				Three-component photoinitiating system				Two-component photoinitiating system				Three-component photoinitiating system			
A	B	A	B	A	B	A	B	A	B	A	B	A	B	A	B
+Iod	+Iod	+NPG	+NPG	+EDB	+EDB	+Iod/NPG	+Iod/NPG	+Iod	+Iod	+NPG	+NPG	+EDB	+EDB	+Iod/NPG	+Iod/NPG
40% ^a	n.p. ^a	n.p. ^a	n.p. ^a	n.p. ^a	n.p. ^a	56% ^b	47% ^b	45% ^a	58% ^a	n.p. ^a	n.p. ^a	n.p. ^a	n.p. ^a	81% ^b	93% ^b

n.p.: no polymerization

a: coumarin/additive: 0.2%/1% w/w

b: coumarin/additives: 0.2%/1%/1% w/w

3.4. Free radical photopolymerization of methacrylates (BisGMA/TEGDMA)

In this part, a comparative study for the different Coumarin/Iod couples is given for the FRP of a benchmarked methacrylate resin (BisGMA/TEGDMA 70%/30% w/w). Typical methacrylate function conversion-time profiles are given in Figure 5 and the FCs are summarized in Table 4. As expected, Iod alone is not able to initiate the polymerization of methacrylates in line with its lack of absorption for $\lambda > 300$ nm, again showing the huge role of these coumarin derivatives for the access to efficient systems.

The CoumB/Iod two-component PIS shows a noteworthy efficiency: FC \square 57% > FC of CoumA/Iod \square 36% (Figure 5, curve 5 vs curve 1, respectively; Table 4). CoumB exhibits a superiority over CoumA, this can be probably ascribed to the slight oxygen inhibition time for polymerization under air, which is observed for CoumA in thick films.

In addition, some photos of BisGMA/TEGDMA thick films (1.4 mm) upon irradiation with the LED@405 nm for 150 s in the presence of Coumarin/Iod two-component photoinitiating systems under air before and after polymerization are shown in Figure S3. Remarkably, a tack free polymer is obtained when using CoumB as PI. In both cases, the color of the obtained polymer remains dark suggesting rather poor bleaching properties during the polymerization.

When Iod is replaced by an amine such as NPG or EDB, the Coumarin/NPG (or EDB) (0.2%/1% w/w) systems show no efficiency using LED@405 nm (Figure 5, curves 2&4 for CoumA and curves 6&8 for CoumB, respectively). Again, the photo-oxidative process in Coumarin/Iod couples shows preponderance over the photo-reductive process in Coumarin/amine (NPG or EDB), for which no polymerization occurs (Figure 5, Table 4).

For the three-component systems Coumarin/Iod/NPG (0.2%/1%/1% w/w), the addition of the amine (NPG) as a hydrogen donor show rather similar polymerization profiles than those obtained for the two-component system Iod/NPG (1%/1% w/w) (Figure 5: curves 3 for CoumA and 7 for CoumB vs. curve 9 for Iod/NPG, respectively). This trend indicates that the coumarin derivatives are less important for methacrylates polymerization in thick films when using three-component PISs.

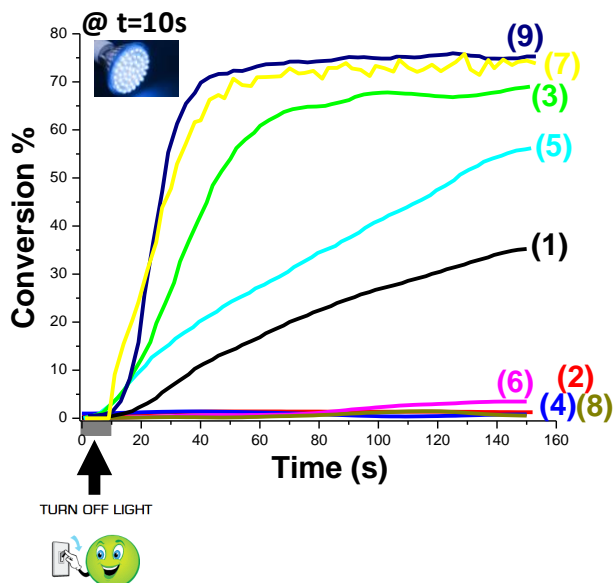


Figure 5. Polymerization profiles (methacrylate function conversion vs. irradiation time) for a BisGMA-TEGDMA blend under air (thickness=1.4 mm) upon exposure to LED@405 nm in the presence of the two and three-component photoinitiating systems: (1) CoumA/Iod (0.2%/1% w/w); (2) CoumA/NPG (0.2%/1% w/w); (3) CoumA/Iod/NPG (0.5%/1%/1% w/w); (4) CoumA/EDB (0.2%/1% w/w); (5) CoumB/Iod (0.2%/1% w/w); (6) CoumB/NPG (0.2%/1% w/w); (7) CoumB/Iod/NPG (0.2%/1%/1% w/w); (8) CoumB/EDB (0.2%/1% w/w) and (9) Iod/NPG (1%/1% w/w); respectively. The irradiation starts for t = 10 s.

Table 4. Reactive Methacrylate Function Conversion (FC) for a BisGMA/TEGDMA blend after 150 s of Irradiation with LED @405 nm Using Different Photoinitiating Systems (under Air; thickness= 1.4 mm); A = CoumA and B = CoumB.

Two-component photoinitiating system (PIS)						Three-component photoinitiating system (PIS)	
Coumarin/Iod or Coumarin/amine (NPG or EDB)						Coumarin/Iod/NPG	
A	B	A	B	A	B	A	B
+Iod	+Iod	+NPG	+NPG	+EDB	+EDB	+Iod/NPG	+Iod/NPG
36% ^a	57% ^a	n.p. ^a	n.p. ^a	n.p. ^a	n.p. ^a	69% ^b	74% ^b

n.p.: no polymerization

a: coumarin/additive: 0.2%/1% w/w

b: coumarin/additives: 0.2%/1%/1% w/w

3.5. 3D printing experiments using Coumarin/Iod & Coumarin/Iod/NPG Systems

Some 3D printing experiments upon laser diode at 405 nm were successfully performed under air using different Coumarin/Iod and/or Coumarin/Iod/NPG systems in TMPTA, BisGMA/TEGDMA or in EPOX/TMPTA (Figure 6). Indeed, the high photosensitivity of these resins (see above) allows an efficient polymerization process in the irradiated area in 3D experiments. Thick polymer samples were obtained with high spatial resolution and very short writing time (~ 1 min). 3D written patterns are characterized by numerical optical microscopy in Figure 6.

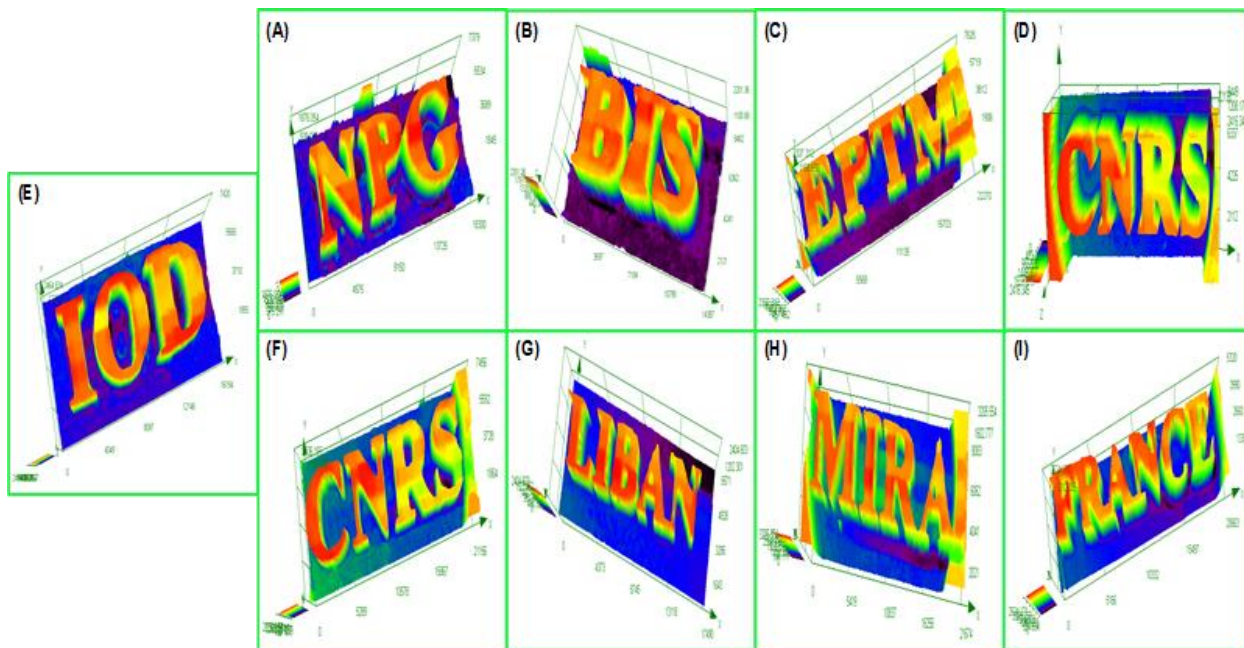


Figure 6. Free radical photopolymerization experiments for 3D printing upon laser diode @405 nm: Characterization of the patterns by numerical optical microscopy; **(A)**: ComB/Iod/NPG (0.012%/0.061%/0.061% w/w) in BisGMA/TEGDMA (thickness = 1880 μm); **(B)**: CoumA/Iod/NPG (0.025%/0.125%/0.125% w/w) in BisGMA/TEGDMA (thickness = 2200 μm); **(C)**: CoumA/Iod (0.04%/0.2% w/w) in EPOX/TMPTA (thickness = 2340 μm); **(D)**: CoumA/Iod (0.05%/0.25% w/w) in TMPTA (thickness = 2420 μm); **(E)**: CoumB/Iod (0.015%/0.077% w/w) in BisGMA/TEGDMA (thickness = 2460 μm); **(F)**: CoumA/Iod (0.04%/0.2% w/w) in TMPTA

(thickness = 2840 μm); **(G)**: CoumB/Iod/NPG (0.018%/0.091%/0.091% w/w) in TMPTA (thickness = 2400 μm); **(H)**: CoumA/Iod/NPG (0.02%/0.1%/0.1% w/w) in TMPTA (thickness = 3200 μm); and **(I)**: CoumB/Iod (0.05%/0.025% w/w) in TMPTA (thickness = 2620 μm); respectively.

3.6. Photopolymerization in water for hydrogels synthesis using CoumB/MDEA:

As CoumB has shown a good efficiency in radical polymerization and is water soluble, the following section focuses on the use of CoumB for the formation of hydrogels which have become very popular due to their unique properties (softness, flexibility and biocompatibility).

In this work, the hydrogels were prepared from the photopolymerization of HEA or HEMA in water (50% water/50% HEMA or HEA) upon LED@405 nm in presence of CoumB/MDEA (0.2%/1% w/w) (Figure 7). The mixture was first degassed by nitrogen (N_2) bubbling in order to reduce the oxygen inhibition. Remarkably, CoumB is very soluble in water compared to its rather low solubility in organic resins such as TMPTA and accordingly is characterized by very high molar extinction coefficients (ϵ) in water (Figure S4). This behavior demonstrates that CoumB can be considered as an excellent water soluble photoinitiator for the production of hydrogels. The generated hydrogels were analyzed by thermogravimetric analysis TGA (Figure 8). The results obtained for CoumB/MDEA (0.2%/1% w/w) system show a loss of water of 78%.

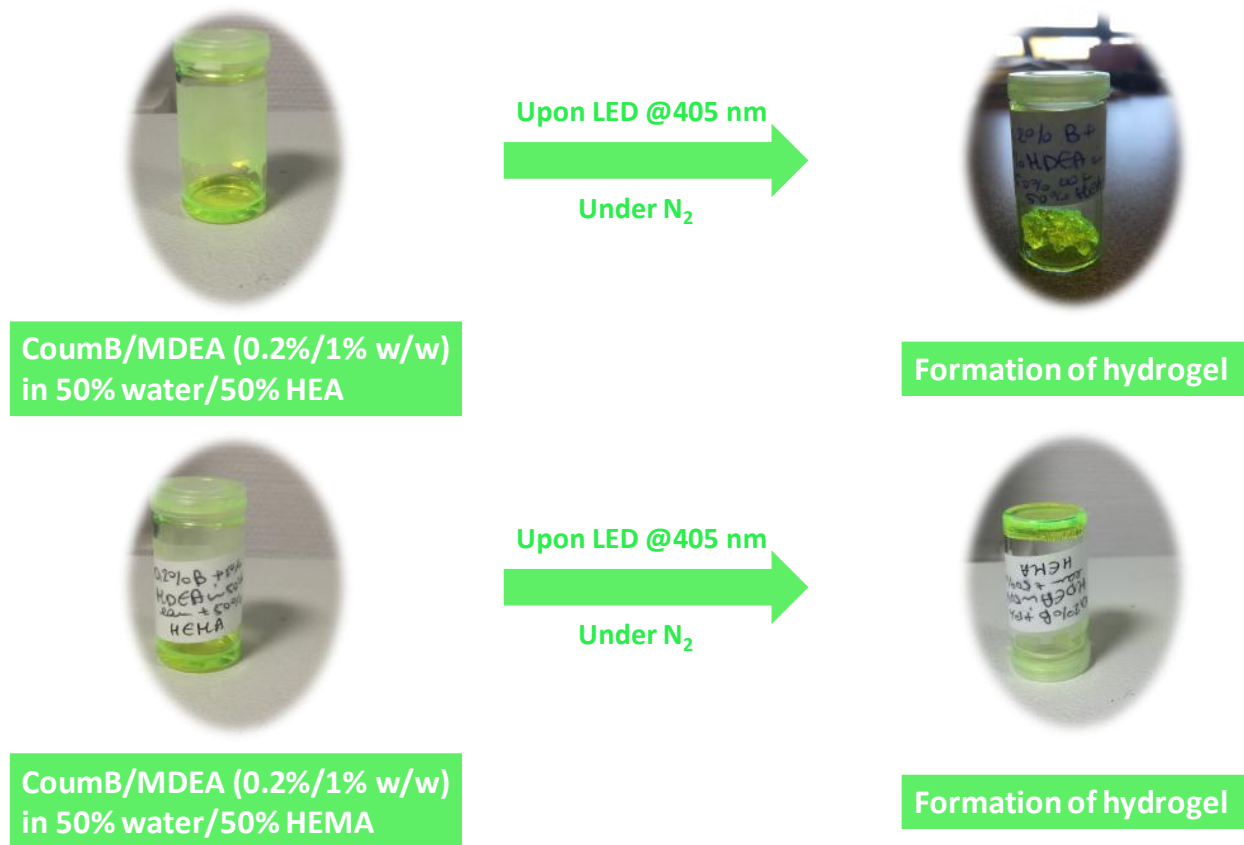


Figure 7. Hydrogels formation using CoumB/MDEA system under N_2 , upon irradiation with LED @405 nm.

3.7. Near-UV conveyor experiments for the access to photocomposites

The current photocomposites were synthesized by impregnation of glass fibers by an organic resin (50% glass fibers/50% resin; thickness of the composite = 2 mm) and then irradiating the sample; BisGMA/TEGDMA (70%/30% w/w) or TMPTA were used as organic resins. The results show that the coumarin derivatives were able to fully cure composites, a very fast curing polymerization was observed i.e. the surface became tack-free after only one pass (for 2 m/min belt speed) of irradiation with a LED@395 nm (Figure 8 and Figure S5), and within one or few

passes on the bottom of the sample, using one layer of glass fibers (thickness = 2 mm). The results are summarized in Table 5.

Furthermore, we note that no significant change of the color of the initial composition was observed using coumarin derivatives, but sometimes a brown color appeared. This behavior demonstrates that the coumarin derivatives exhibit an outstanding reactivity for the production of composite materials with an excellent depth of cure upon near-UV light.



Figure 8. Composite produced upon Near-UV light (LED@395 nm), Belt Speed = 2m/min, using the free radical **polymerization** (FRP) in the presence of glass fibers/acrylate resin (0.2% CoumB + 1% Iod + 1% NPG in TMPTA). Glass fibers: ~ 2mm of thickness for one layer; 50% glass fibers/50% organic resin.

Table 5. Number of passes to be tack-free for impregnated glass fibers with (meth)acrylate resins using Near-UV conveyor (LED @395 nm), belt speed used = 2 m.min⁻¹

One layer of glass fibers (50% glass fibers/50% (meth)acrylate resin)	At the surface	On the bottom
0.2% CoumB + 1% Iod + 1% NPG in TMPTA	T.F. after 1 pass	T.F. after 1 pass

0.2% CoumB + 1% Iod + 1% NPG in BisGMA/TEGDMA	T.F. after 1 pass	T.F. after 1 pass
0.2% CoumB + 1% Iod in BisGMA/TEGDMA	T.F. after 1 pass	T.F. after 7 passes
0.2% CoumA + 1% Iod + 1% NPG in BisGMA/TEGDMA	T.F. after 1 pass	T.F. after 2 passes
0.2% CoumA + 1% Iod + 1% NPG in TMPTA	T.F. after 1 pass	T.F. after 8 passes

T.F.: Tack-free

3.8. Chemical Mechanisms

3.8.1. Steady State Photolysis

Steady state photolysis experiments for the different initiating systems have been carried out. The photolysis of CoumA/Iod in acetonitrile upon irradiation with a LED@ 375 nm is very fast compared to that of CoumA alone (Figure 9B vs. Figure 9A). A new photoproduct (characterized by a significant new absorption for $\lambda > 470$ nm) is formed in any case which, accordingly, is due to the CoumA/Iod interaction. Accordingly, it is noteworthy to mention that the photobleaching character is in line with the high reactivity/efficiency of this system in polymerization. Indeed, the degradation of CoumA is clearly shown in Figure 9C, where the optical density of the solution is measured vs. irradiation time in the presence of Iod (Figure 9C, curve 2) and without addition of Iod (Figure 9C, curve 1). The photolysis of CoumB in presence of Iod is also much faster than that for CoumB alone also suggesting a strong CoumB/Iod interaction.

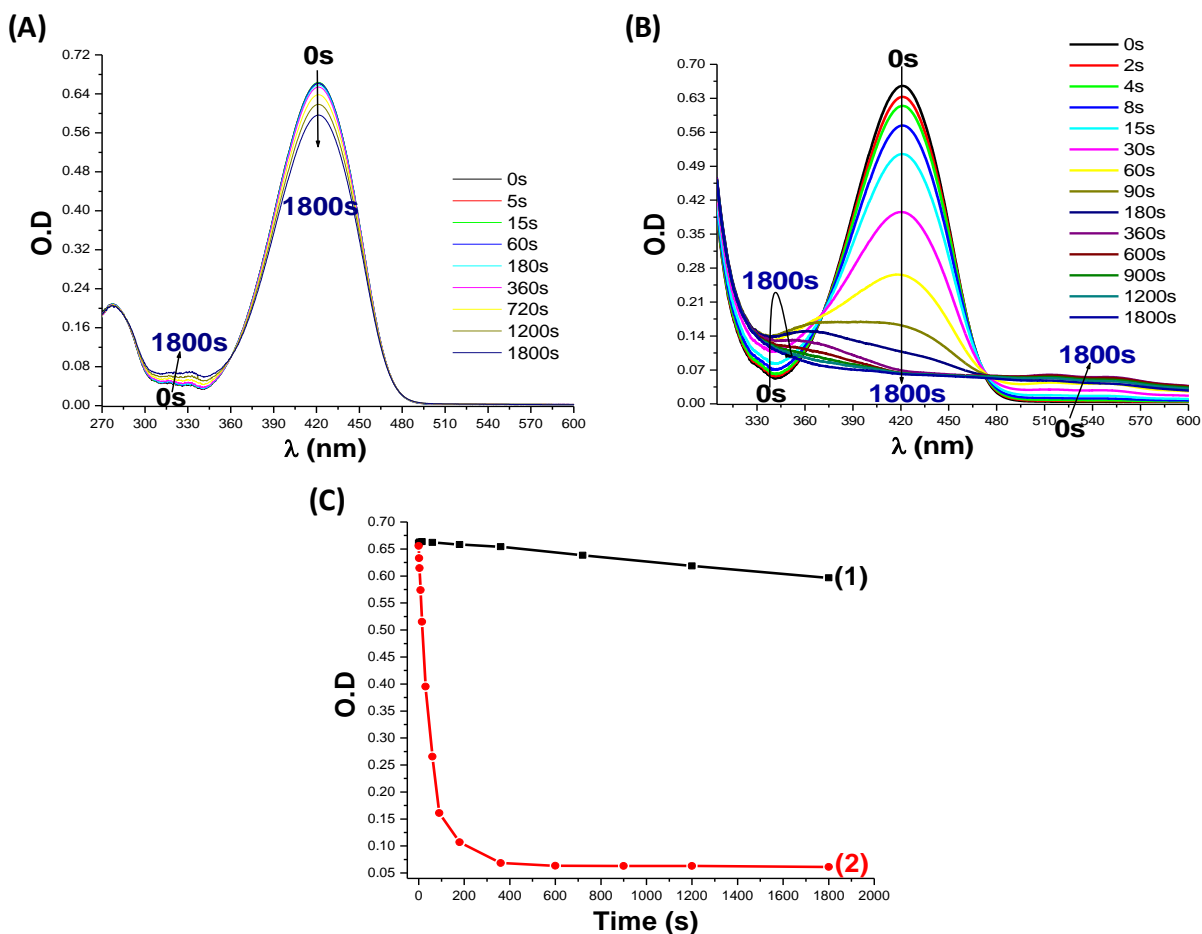


Figure 9. (A): Photolysis of CoumA in absence of Iod; **(B):** CoumA/Iod photolysis; and **(C):** Degradation of CoumA without (1) and with (2) Iod vs. irradiation time. Upon exposure with LED@375 nm in ACN.

3.8.2. Fluorescence quenching, Cyclic Voltammetry and ESR Experiments

Fluorescence and fluorescence quenching experiments in acetonitrile for the coumarin derivatives are shown in 10. First, the crossing point of the absorption and fluorescence spectra allows the determination of the singlet excited state energy (E_{S1}) for CoumA and CoumB (Figure 10A); $E_{S1} = 2.68$ V for CoumA and 2.72 V for CoumB in full agreement with [9]; Table 6).

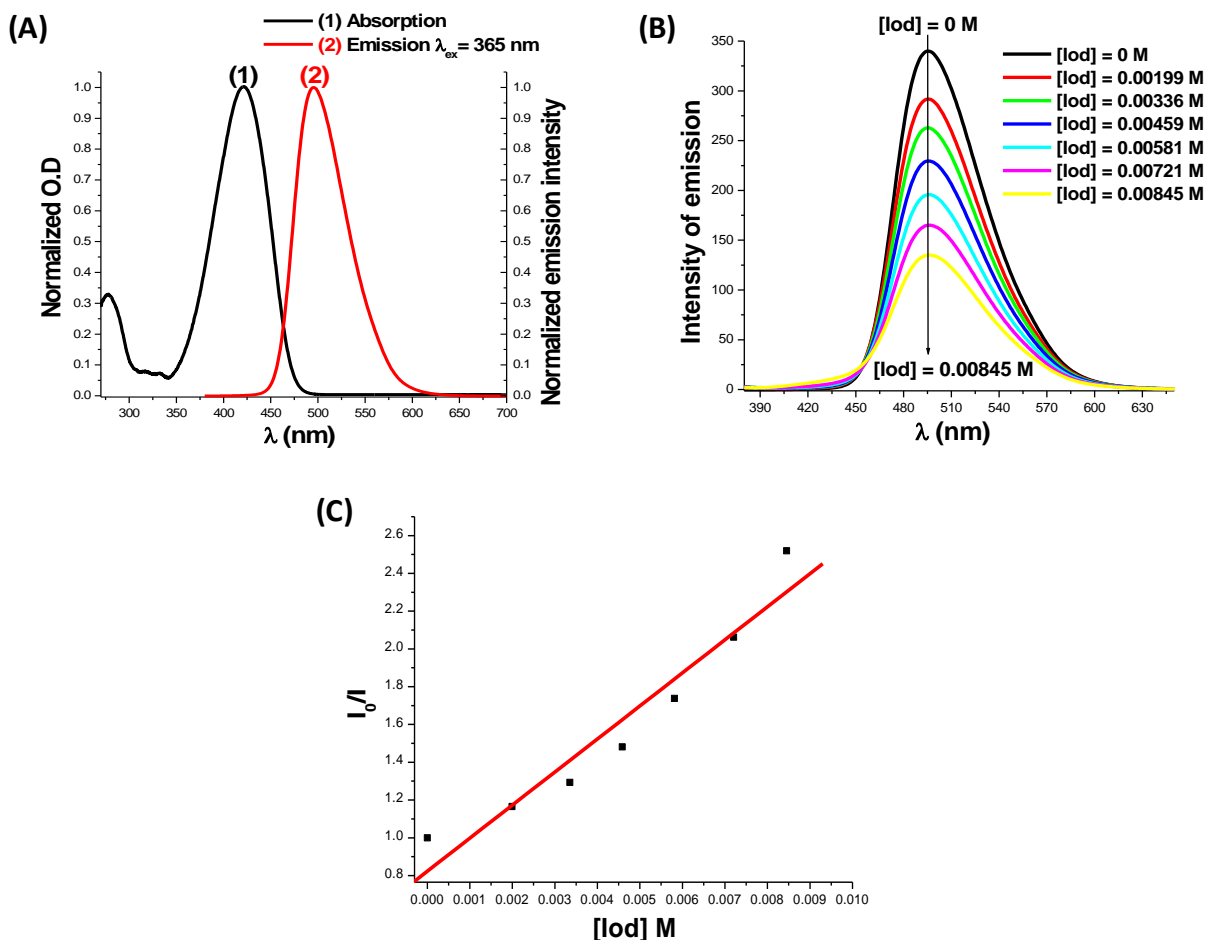


Figure 10. (A): Singlet state energy determination in acetonitrile for CoumA; (B): Fluorescence quenching of CoumA/Iod; and (C): Stern–Volmer treatment for the CoumA/Iod fluorescence quenching.

Table 6. Parameters Characterizing the Chemical Mechanisms Associated with ^{1,3}Coumarin/Iod in Acetonitrile.

PI/Iod	E_{ox} (eV)	E_{S1} (eV)	$\Delta G_{et(S1)}$ (Coumarin/Iod) (eV)	E_{T1} (eV)	$\Delta G_{et(T1)}$ (Coumarin/Iod) (eV)
CoumA/Iod	0.81	2.68	-1.67	1.81	-0.8
CoumB/Iod	0.8	2.72	-1.72	1.56	-0.56

The free energy changes (ΔG_{et}) for the electron transfer reaction between Coumarins as electron donors and Iod as an electron acceptor were calculated from the classical equation (eq 1) using the oxidation potentials E_{ox} and the excited state energies E_{S1} of coumarins (Table 6). Favorable $^1\text{CoumA}$ (or $^1\text{CoumB}$)/Iod fluorescence quenching processes were shown in full agreement with highly favorable ΔG_{et} (reactions r1 & r2 – Scheme 4; e.g., for CoumA/Iod, $\Delta G_{et} = -1.67$ eV; Table 6).

A triplet state pathway cannot be ruled out (triplet state energy calculated from molecular orbital calculations (uB3LYP/6-31G* level of theory; Table 6) i.e. the favorable free energy changes ($\Delta G_{et(T1)}$) for $^3\text{Coumarin}$ /Iod are also favorable (Table 6).

A global mechanism is proposed in reactions r1-r8 (Scheme 4). Coumarin/Iod interaction is proposed to occur thanks to the classical [24] reduction of the iodonium salt (r1 and r2) (see above, the favorable ΔG and the fluorescence quenching data). This is also confirmed by Electron Spin Resonance (ESR) results. Indeed, Spin trapping experiments using phenyl-*N-tert*-butylnitron (PBN) is an efficient technique to characterize the generated radicals. In agreement with r2, the irradiation of a CoumA (or CoumB) solution in the presence of Iod and PBN generates aryl (Ar^\bullet)/PBN radical adducts which are easily detected in ESR-ST experiments and characterized by hyperfine coupling constants (*hfc*s): $a_N = 14.3$ G and $a_H = 2.2$ G [25].

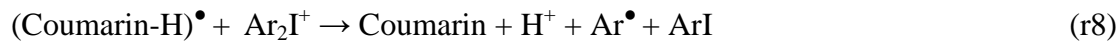
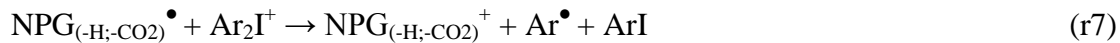
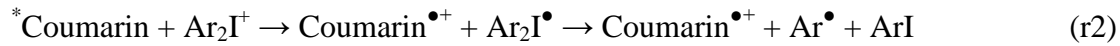
The aryl radicals are excellent initiating species for addition onto (meth)acrylate double bond ($k_{add} = 10^8 \text{ M}^{-1} \cdot \text{s}^{-1}$) [26] in full agreement with the good efficiency of the Coumarin/Iod couples.

Finally, it is proposed that NPG which is an *N*-aromatic electron donor can form a Charge Transfer Complex (CTC) with an electron poor iodonium salt (r3) as what was very recently

published [27]. An example of **similar *N*-aromatic** amine/iodonium salt CTC structure is available in the literature [27]. This [NPG-Iod]_{CTC} structure is quite convenient as it provides an enhanced visible light absorption to the photoinitiating system, and the photolysis at 405 nm leads to an efficient release of Ar[•] radicals (r4) as confirmed by the photopolymerization study (curve (9) in Figures 4(A), 4(B), and Figure 5).

Then, the Coumarin/NPG interaction can correspond to an electron/proton transfer reaction (r1 and r5). Then, a proposed decarboxylation reaction in NPG (r6) leading to NPG_(-H;-CO2)[•] is responsible to avoid any back electron transfer reaction. NPG_(-H;-CO2)[•] can be considered as the initiating species for the free radical polymerization in Coumarin/NPG systems even if this process is not very efficient (see above the low initiating ability of Coumarin/NPG).

For the three-component system, we propose that r7 and r8 occur as in other previously studied dye/amine/iodonium salt systems [27]. Therefore, NPG_(-H;-CO2)[•], Ar[•] and Coumarin^{•+}, NPG_(-H;-CO2)⁺ can be considered as the initiating species for FRP and for CP, respectively.



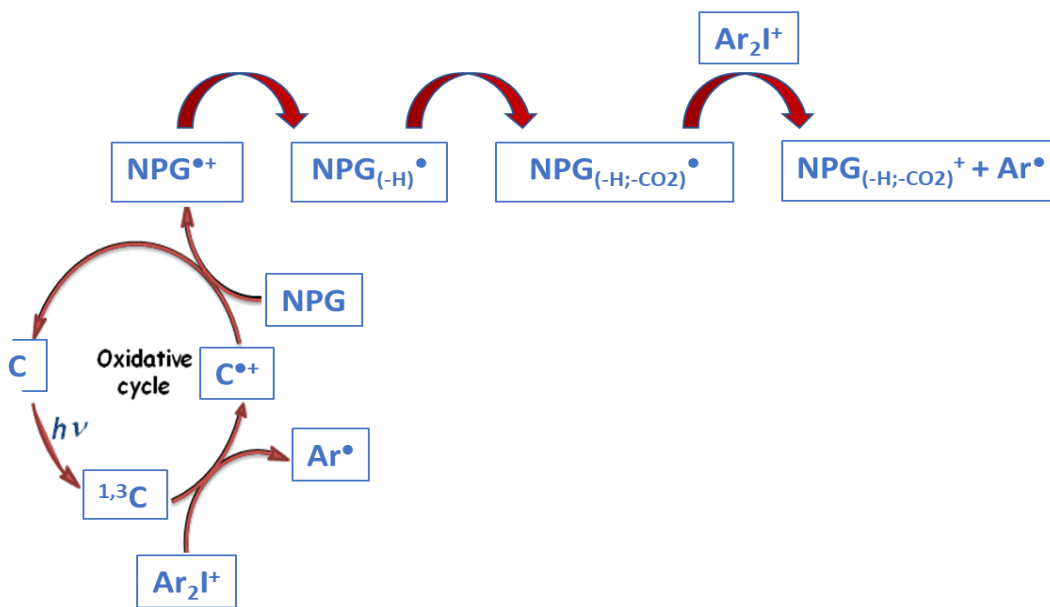
Scheme 4. Proposed chemical mechanisms for photoinitiated polymerization by CoumA or CoumB.

3.8.3. Coumarin derivatives as Photoredox Catalysts in Three-Component System

The CoumA/Iod/NPG three-component PIS works according to Scheme 5 through mainly an oxidative cycle as the Coumarin/Iod interaction is much more efficient than Coumarin/amine.

First, the Coumarin reacts with the iodonium salt to form the oxidized form that can latter react with the NPG to be regenerated through a photoredox catalytic cycle presented in Scheme 5.

The concomitant regeneration of coumarins ensures a photoredox catalyst behaviour in line with the observed improved efficiency of the polymerization (Coumarin/Iod/NPG better than Coumarin/Iod). This behaviour is also observed in steady state photolysis where the consumption of coumarin achieved with three-component PISs (Coumarin/Iod/NPG) is lower than that reached when using two-component PISs based on Coumarin/Iod combinations showing a partial regeneration e.g., Consumption % of CoumA = 54% with CoumA/Iod/NPG vs. 90% with CoumA/Iod (Figure 11A, curve 3 vs. curve 2, respectively).



Scheme 5. Proposed oxidative cycle for Coum/Iod/NPG systems.

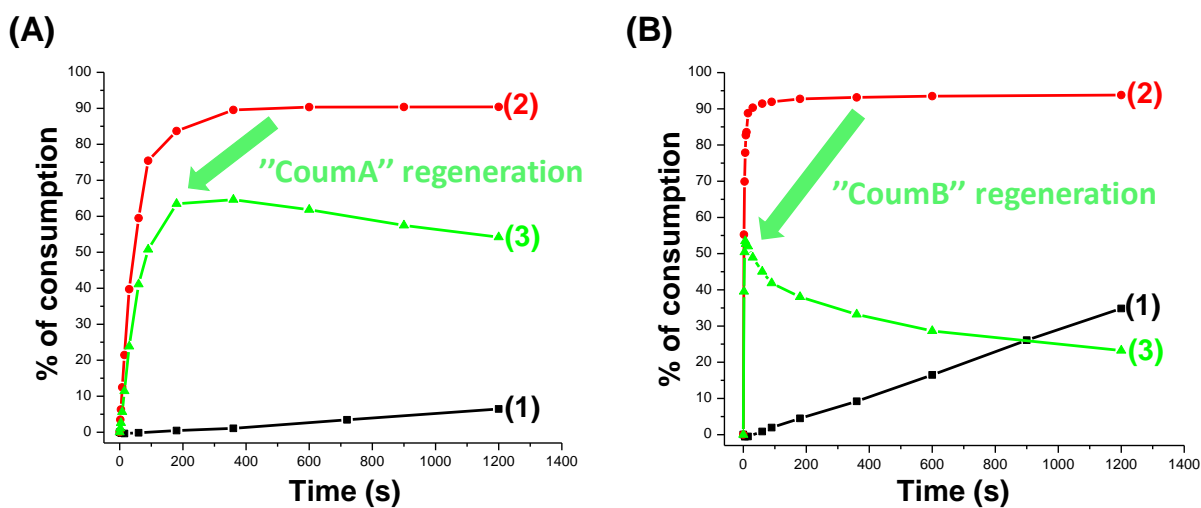


Figure 11. Consumption of CoumA (A) or CoumB (B); (1) without Iod salt; (2) with Iod salt; and (3) with Iod salt + NPG, vs time of irradiation with LED@375 nm.

4. Conclusion

In the present paper, coumarin derivatives characterized by strong visible light absorptions are proposed for the development of new high performance photoinitiators/photoredox catalysts for the photoinitiation of both the cationic polymerization of epoxides and the free radical polymerization of (meth)acrylates upon violet and blue LEDs. Both high final conversions and polymerization rates are obtained. These coumarin derivatives are efficient photoredox catalysts because these compounds combine suitable oxidation potentials at the excited state, highly favorable free energy changes ΔG_{et} and good absorbance under LED@405 nm exposure. The high performance of these coumarin derivatives (CoumA; CoumB) in initiating systems is also shown for new photosensitive 3D printing resins upon exposure to laser diode but also when used LED projector at 405 nm. One of these new photoinitiators (CoumB) was also successfully used for the preparation of hydrogels due to its high solubility in water. These new initiating systems were also used for the synthesis of photocomposites. The developments of high performance photosensitive systems in water will be presented in forthcoming papers.

Acknowledgments:

The Lebanese group would like to thank “The Association of Specialization and Scientific Guidance” (Beirut, Lebanon) for funding and supporting this scientific work. Cyanagen s.r.l. is acknowledged for the supply of coumarins dyes and for financial support to G.C.

Supporting Information: Synthetic procedure for CoumA and CoumB; Figure S1: Color before and after photopolymerization for CoumA in EPOX; Figure S2: Color before and after

photopolymerization for the different polymers in TMPTA; Figure S3: Color before and after photopolymerization for the different polymers in BisGMA/TEGDMA; Figure S4: Absorption spectrum of CoumB in water; and Figure S5: Synthesis of photocomposites (thickness = 2 mm) upon Near-UV light (LED @395 nm), Belt Speed = 2m/min, using the free radical **polymerization** (FRP) in the presence of glass fibers/(meth)acrylate resin for different systems based on coumarin derivatives.

REFERENCES:

- [1] K. Hunger, *Industrial Dyes*, WILEY-VCH Verlag, Gmbh & Co. KGaA, Weinheim, Germany, 2003.
- [2] A. Dmitry, A. Pavel, Dipyrrolyl quinoxalines with extended chromophores are efficient fluorimetric sensors for pyrophosphate, *Chemical Communications* 12 (2003) 1394–1395.
- [3] H. Gold, in: H. Venkataraman (Ed.), *The Chemistry of Synthetic Dyes*, Pergamon, Academic Press, New York, USA, 1971, pp. 535–542.
- [4] E. Belgodere, R. Bossio, S. Chimichi, V. Passini, R. Pepino, Synthesis and fluorescence of some thiazole and benzothiazole derivatives, *Dyes and Pigments* 4 (1985) 59–71.
- [5] A.G. Kalle, British Patent 1962, 895 (001).
- [6] a) H. Li, L. Cai, J. Li, Y. Hu, P. Zhou and J. Zhang, *Dyes and Pigments*, 2011, 91, 309-316; b) B. B. Raju and T. S. Varadarajan; *Laser Chem.* 1995, 16, 109–120; c) M. Fujiwara, N. Ishida, M. Satsuki and S. Suga, *J Photopolym. Sci. Technol.* 2002, 15, 237–238; d) K. Hara, Z.-S. Wang, T. Sato, A. Furube, R. Katoh, H. Sugihara, Y. Dan-oh, C. Kasada, A. Shinpo and S. Suga, *J. Phys. Chem. B* 2005, 109, 15476-15482.
- [7] Specht, D. P.; Matric, P. A.; Farid, S. *Tetrahedron* 1982,38,1203-1211. Specht, D. P.; Houle, C. G.; Faird, S. Y. U.S. Patent 4 289 844,1981; *Chem. Abstr.* 1981, 94,46756~.
- [8] Monroe, Bruce M. and Weed, Gregory C., Photoinitiators for free-radical-initiated photoimaging systems, *Chemical Reviews*, Vol. 93, number 1, pages 435-448, year 1993, 10.1021/cr00017a019.
- [9] Gualandi, A., Rodeghiero, G., Della Rocca, E., Bertoni, F., Marchini, M., Perciaccante, R., Jansen, T.P., Ceroni, P. and Cozzi, P.G., Application of coumarin dyes for organic photoredox

catalysis. *Chemical Communications*, 54(72), pp.10044-10047, July 2018, 10.1039/C8CC04048F.

[10] S.-M. Yang, C.-Y. Wang, C.-K. Lin, P. Karanam and G. M. Reddy, *Angew. Chem. Int. Ed.* 2018, 57, 1668-1672.

[11] M. Ozkütük, E. Ipek, B. Aydiner, S. Mamas and Z. Seferoglu, *J.Mol. Struct.* 2016, 108, 521-532.

[12] Chirani, Naziha & Yahia, L'Hocine & Gritsch, Lukas & Motta, Federico & Chirani, Soumia & Farè, Silvia. (2015). History and Applications of Hydrogels. *Journal of Biomedical Sciences*. Vol. 4. 13-23. 10.4172/2254-609X.100013.

[13] Enrica Caló, Vitaliy V. Khutoryanskiy, Biomedical applications of hydrogels: A review of patents and commercial products, *European Polymer Journal*, Vol. 65, Pages 252-267, April 2015.

[14] Lindsey A Sharpe and Adam M Daily and Sarena D Horava and Nicholas A Peppas, Therapeutic applications of hydrogels in oral drug delivery, *Expert Opinion on Drug Delivery*, Vol. 11, number 6, pages 901-915, year 2014, publisher Taylor & Francis, doi = 10.1517/17425247.2014.902047.

[15] Enas M. Ahmed , Hydrogel: Preparation, characterization, and applications: A review, *Journal of Advanced Research*, Vol. 6, Issue 2, Pages 105-121, March 2015.

[16] C. Dietlin, S. Schweizer, P. Xiao, J. Zhang, F. Morlet-Savary, B. Graff, J.P. Fouassier, J. Lalevée, Photopolymerization upon LEDs: New Photoinitiating Systems and Strategies. *Polym. Chem.* 6 (2015) 3895–3912.

- [17] J. Lalevée, N. Blanchard, M.A. Tehfe, F. Morlet-Savary, J.P. Fouassier, Green Bulb Light Source Induced Epoxy Cationic Polymerization under Air Using Tris(2,2'-bipyridine)ruthenium(II) and Silyl Radicals. *Macromolecules* 43 (2010) 10191–10195.
- [18] J. Lalevée, N. Blanchard, M.A. Tehfe, M. Peter, F. Morlet-Savary, D. Gigmes, J.P. Fouassier, Efficient Dual Radical/Cationic Photoinitiator under Visible Light: A New Concept. *Polym. Chem.* 2 (2011) 1986–1991.
- [19] D. Rehm, A. Weller, A. Kinetics of Fluorescence Quenching by Electron and H-Atom Transfer. *Isr. J. Chem.* 8 (1970) 259–271.
- [20] J.B. Foresman, A. Frisch, *Exploring Chemistry with Electronic Structure Methods*, 2nd ed.; Gaussian Inc.: Pittsburgh, PA, 1996.
- [21] Frisch, M. J.; Trucks, G.W.; Schlegel, H. B.; Scuseria, G. E.; Robb, M. A.; Cheeseman, J. R.; Zakrzewski, V. G.; Montgomery, J. A.; Stratmann, J. R. E.; Burant, J. C.; Dapprich, S.; Millam, J.M.; Daniels, A. D.; Kudin, K. N.; Strain, M. C.; Farkas, O.; Tomasi, J.; Barone, V.; Cossi, M.; Cammi, R.; Mennucci, B.; Pomelli, C.; Adamo, C.; Clifford, S.; Ochterski, J.; Petersson, G. A.; Ayala, P. Y.; Cui, Q.; Morokuma, K.; Salvador, P.; Dannenberg, J. J.; Malick, D. K.; Rabuck, A. D.; Raghavachari, K.; Foresman, J. B.; Cioslowski, J.; Ortiz, J. V.; Baboul, A. G.; Stefanov, B. B.; Liu, G.; Liashenko, A.; Piskorz, P.; Komaromi, I.; Gomperts, R.; Martin, R. L.; Fox, D. J.; Keith, T.; Al-Laham, M. A.; Peng, C. Y.; Nanayakkara, A.; Challacombe, M.; Gill, P. M. W.; Johnson, B.; Chen, W.; Wong, M.; Andres, J. L.; Gonzalez, C.; Head-Gordon, M.; Replogle, E. S.; Pople, J. A. *Gaussian 03, Revision B-2*; Gaussian Inc.: Pittsburgh, PA, 2003.
- [22] J. Zhang, F. Dumur, P. Xiao, B. Graff, D. Bardelang, D. Gigmes, J.P. Fouassier, J. Lalevee, Structure Design of Naphthalimide Derivatives: Toward Versatile Photoinitiators for Near-

UV/Visible LEDs, 3D Printing, and Water-Soluble Photoinitiating Systems *Macromolecules* 48 (2015) 2054–2063.

[23] P. Xiao, F. Dumur, J. Zhang, J.P. Fouassier, D. Gigmes, J. Lalevee, Copper Complexes in Radical Photoinitiating Systems: Applications to Free Radical and Cationic Polymerization upon Visible LEDs. *Macromolecules* 47 (2014) 3837–3844.

[24] N. Zivic, M. Bouzrati-Zerelli, A. Kermagoret, F. Dumur, J.P. Fouassier, D. Gigmes, J. Lalevée, Photocatalysts in polymerization reactions. *ChemCatChem* 8 (2016) 1617–1631.

[25] J. Lalevee, J.-P. Fouassier, *Dyes and Chromophores in Polymer Science*, Wiley-ISTE, London, 2016.

[26] J.-P. Fouassier, J. Lalevee, *Photoinitiators for Polymer Synthesis, Scope, Reactivity, and Efficiency*; Wiley-VCH Verlag GmbH & Co.KGaA: Weinheim, 2012.

[27] P. Garra, B. Graff, F. Morlet-Savary, C. Dietlin, J.M. Becht, J.P. Fouassier, J. Lalevée, Charge Transfer Complexes as Pan-Scaled Photoinitiating Systems: From 50 μm 3D Printed Polymers at 405 nm to Extremely Deep Photopolymerization (31 cm) *Macromolecules* 51 (2018) 57–70.

TOC graphic:

